

See discussions, stats, and author profiles for this publication at: <https://www.researchgate.net/publication/231685489>

Optimum toughening of homopolymer interfaces with block copolymers

ARTICLE *in* MACROMOLECULES · OCTOBER 1993

Impact Factor: 5.8 · DOI: 10.1021/ma00074a025

CITATIONS

37

READS

24

5 AUTHORS, INCLUDING:



[Costantino Creton](#)

École Supérieure de Physique et de Chimie In...

215 PUBLICATIONS 4,188 CITATIONS

[SEE PROFILE](#)

Optimum Toughening of Homopolymer Interfaces with Block Copolymers

Junichiro Washiyama,[†] Costantino Creton,[‡] and Edward J. Kramer*

Department of Materials Science and Engineering and the Materials Science Center,
Cornell University, Ithaca, New York 14853

Fei Xiao and Chung-Yuen Hui

Department of Theoretical and Applied Mechanics and the Materials Science Center,
Cornell University, Ithaca, New York 14853

Received March 1, 1993; Revised Manuscript Received June 30, 1993*

ABSTRACT: We have investigated the fracture toughness and fracture mechanisms of planar interfaces between polystyrene (PS) and poly(2-vinylpyridine) (PVP), which were reinforced with a series of deuterium-labeled dPS-PVP block copolymers of relatively high areal chain density, Σ : these are designated 800/870, 510/540, and 580/220, where the numbers are the polymerization indices of the dPS and PVP blocks. The critical energy release rate of the interfacial crack, G_c (fracture toughness), was measured as a function of Σ using an asymmetric double cantilever beam geometry, and fracture mechanisms were studied by transmission electron microscopy (TEM) and forward recoil spectrometry (FRES), which permitted the location of the dPS block to be determined. For the asymmetric block copolymer (580/220), we observed spherical micelles on the PS side of the interface at large Σ 's and G_c remained constant, indicating that these block copolymer micelles have no effect on G_c . FRES and TEM observations showed that fracture occurred by crazing in PS followed by craze breakdown, and the locus of the fracture was the PVP/PS craze interface. In contrast to these results for the asymmetric block copolymer, we observed that the symmetrical block copolymers (510/540 and 800/870) formed lamellae at the interface at large Σ 's and that this lamellar structure affected G_c . In both cases, after exhibiting a maximum at Σ corresponding to the saturation coverage of the interface with block copolymer chains, G_c began to decrease and finally reached a constant value when the interface was fully covered with one additional block copolymer lamella. TEM observation showed that the fracture mechanism is crazing on the PS side followed by craze breakdown at the PVP/PS craze interface. FRES analysis revealed that for 800/870 fracture took place both within the PS lamella and at the interface between outer block copolymer chains of the lamella and PS homopolymer, while fracture took place between the dPS block brush at the saturated interface and the dPS block of the lamella for 510/540. These results show that there are limits to the interface toughening that can be produced by adding diblock copolymers, especially for symmetric block copolymers. Adding more block copolymer than needed to saturate the interface actually produces secondary (lamellar) interfaces which are weaker than the original saturated homopolymer one.

Introduction

Good adhesion between different phases in phase-separated polymer blends and laminates is important for the mechanical performance of these materials. A strategy for achieving this adhesion has been to add small amounts of A-B block copolymers to the mixture of immiscible A and B homopolymers; these block copolymers are known to segregate to the interfaces^{1,2} and, under the right circumstances, this segregation can lead to significant interface reinforcement.³⁻¹⁰

The principal variables governing the adhesion are the areal chain density Σ of the block copolymer at the interface and the polymerization indices (N_A and N_B) of the two blocks. Theoretical considerations,^{5,6,8,9} backed by recent experiments, suggest that the interfaces can fail by several different mechanisms, including the following:

(1) Chain scission of the A-B block copolymer somewhere near its joint if Σ is relatively small and N_A and N_B are relatively large. This failure mechanism can occur without triggering significant crazing or other plastic deformation ahead of the crack tip.

(2) Chain pullout of the shortest block copolymer. This mechanism generally will occur if either N_A or N_B is much

less than $N_{e,A}$ or $N_{e,B}$, respectively, where the N_e 's are the polymerization indices corresponding to the entanglement molecular weights of the respective homopolymers.

(3) Growth of a craze into the homopolymer with the smaller crazing stress σ_{craze} , followed by failure of the craze fibrils near the original interface. The mechanism of fibril failure can be scission of the remaining entangled strands of homopolymer or block copolymer due to the stress concentration which develops within the craze as the craze widens.

Much of the recent advance in this area can be traced to the development of a simple test specimen, a asymmetric double cantilever beam,^{11,12} which can be used to accurately measure the fracture toughness of planar interfaces between immiscible homopolymers.^{4,5,8} The technique for specimen production permits one to place known amounts of the block copolymer at the interface by spin casting before welding two polymer slabs together above their glass transition temperature. If the block copolymer can be labeled with deuterium, forward recoil spectrometry (FRES) and/or dynamic secondary ion mass spectrometry (SIMS) can be used to directly measure Σ . If only one block of the copolymer is deuterated, the fraction of deuterium on each side of the fracture gives important clues as to which of the failure mechanisms outlined above actually operated.^{3,8} And finally, thin microtomed slices can be prepared from such specimens so that cross-sectional transmission electron microscopy of both the unfractured interface and the region of the crack tip can be performed.¹⁰

* Visiting scientist from Kawasaki Plastics Laboratory, Showa Denko K.K., 3-2, Chidori-cho, Kawasaki-ku, Kawasaki, Kanagawa, 210, Japan.

[†] Present address: IBM Almaden Research Center, 650 Harry Rd., San Jose, CA 95120.

• Abstract published in *Advance ACS Abstracts*, September 1, 1993.

Table I. Characterization of Homopolymers and Block Copolymers

homopolymer			block copolymers		
code	M_n	M_w	code	N_{PS}	N_{PVP}
PS ^a	100 000	250 000	580/220	580	220
PVP	80 000	200 000	510/540	510	540
			800/870	800	870

^a The PS block is deuterated.

According to these studies, crazing is necessary to achieve strong interfacial reinforcement with block copolymers, and in this crazing regime, G_c scales as $G_c \sim \Sigma^{2.5,8,9}$ indicating that a larger Σ gives a much stronger interface. The maximum (saturation) Σ is restricted by preferential formation of micelles and lamellae near the interface, which is in turn determined by thermodynamic characteristics, particularly the segregation isotherm and the critical micelle concentration of the block copolymer, which can be determined by FRES and TEM.¹³ It should be noted that the micelles or lamellae which appear beyond saturation can, in principle, affect G_c and the corresponding deformation and fracture mechanisms of the interface. Despite many studies in the relatively low Σ regime, there have been few in the higher Σ one and there is no precise knowledge of how these microdomains affect G_c . While Brown⁴ demonstrated the existence of a maximum in G_c vs Σ using selected symmetric diblock copolymers and conjectured that the subsequent decrease in G_c at values of Σ beyond the maximum was due to the formation of lamellar structures, he was not able to obtain direct evidence to prove his hypothesis. In this paper, we investigate the high Σ regime, beyond interface saturation, in more detail to determine where and how optimum toughening of the interface can be achieved.

We have chosen polystyrene (PS) and poly(2-vinylpyridine) (PVP) homopolymers as the immiscible polymer pair and PS/PVP block copolymers as the compatibilizer to reinforce the interface between PS and PVP. The advantage of this system is that both homopolymers have nearly the same glass transition temperature and mechanical properties; namely, both of them deform plastically by crazing,⁷ which can be easily recognized by transmission electron microscopy (TEM).¹⁰ Furthermore, thermodynamic characteristics, such as the Flory interaction parameter, χ , between PS and PVP and the adsorption isotherm of the block copolymer to the interface are known from previous studies,^{14–16} giving us an additional advantage in understanding this system.

Experimental Section

(1) **Materials.** PS and PVP homopolymers purchased from Aldrich Chemical Co. Inc. were of commercial grade with weight-average molecular weights of 250 000 and 200 000, respectively. The dPS/PVP block copolymers listed in Table I were synthesized by anionic polymerization in tetrahydrofuran using cumyl potassium as the initiator at -55°C in an argon atmosphere. The PS block is deuterium labeled so that the quantity of the PS block at the interface can be analyzed with FRES. The molecular weight and the composition of the block copolymers were characterized using gel permeation chromatography (GPC), forward recoil spectroscopy (FRES),^{17,18} and nuclear magnetic resonance (NMR). The polydispersity indices of these block copolymers were 1.1 or less. The various block copolymers will be designated by their polymerization indices; i.e., the block copolymer whose polymerization index of the dPS block is 580 and that of the PVP block is 220 will be denoted as 580/220. More details of the polymerization and the characterization can be found elsewhere.¹⁹

(2) **Sample Preparation.** A thin film of the block copolymer was spun cast from a toluene solution on a PVP slab. The areal density of block copolymer chains at the interface, Σ , was

controlled by varying the concentration of the block copolymer in solution (0.1–3.0%), which in turn determined the thickness of the initial block copolymer layer. The resulting PVP slab was then joined to a PS slab and annealed in a mold at 160°C for 2 h. In this annealing process, some block copolymer chains diffuse away from the interface, but most block copolymer chains organize themselves at the interface or form micelles or lamellae near the interface. A true equilibrium, which for supersaturated interfaces consists of micelles (lamellae) throughout the PS slab, was not achieved. Nevertheless, we believe that the annealing time was long enough that a (metastable) equilibrium swelling of the lamellae by chains of the homopolymer occurred (see Appendix). The resulting sandwich was then cut with a diamond saw to obtain strips for the subsequent fracture toughness measurement. The dimensions of the strips were 50.8 mm long \times 8.7 mm wide \times 4.0 mm thick (2.3 and 1.7 mm for PS and PVP, respectively). One of these strips was cut into smaller pieces for the microtomy described in the later section.

(3) **Measurement of Fracture Toughness.** The fracture toughness of the interface, G_c , which is defined as the critical energy release rate of an interfacial crack, was measured using an asymmetric double cantilever beam geometry (ADCB).⁸ The measurement was performed by inserting a single-edge razor blade at the interface and pushing it at a constant rate of $3 \times 10^{-6} \text{ m/s}$ using a servo-controlled motor drive at room temperature in air. The steady-state value of the crack length, a , along the interface ahead of the razor blade was measured at a regular interval. The fracture toughness, G_c , which is proportional to a^{-4} ,⁸ was computed using these values of a . The error bars reported subsequently for G_c represent ± 1 standard deviation of at least 16 measurements. After the G_c measurement, the fracture surfaces of the two beams of the ADCB were examined with FRES to determine the areal density of block copolymer chains on both PS and PVP sides ($\Sigma(\text{PS})$ and $\Sigma(\text{PVP})$, respectively). The total areal chain density, Σ , was calculated by summing these two measurements; i.e., $\Sigma = \Sigma(\text{PS}) + \Sigma(\text{PVP})$.

In the PS/PVP system, an asymmetric geometry is necessary to measure the true value of G_c of the interface. Since the modulus of PVP is higher than that of PS, the stress field of the crack is characterized by a complex stress intensity factor $K = K_1 + iK_2$, where $i = (-1)^{1/2}$. Specifically, the traction directly ahead of the crack tip along the interface has both a shear (σ_{xy}) and a tensile (σ_{yy}) component. The ratio of the shear stress to the tensile stress directly ahead of the crack tip at $x = d$, where d is a distance that is small compared to typical specimen dimensions, is related to a phase angle Ψ by:

$$(\sigma_{xy}/\sigma_{yy})_{x=d} = \tan \Psi = \text{Im}(Kd^{ie})/\text{Re}(Kd^{ie}) \quad (1)$$

where ϵ is a dimensionless material parameter which depends on the mismatch of elastic moduli between the two materials on either side of the interface.²⁰ For the PS/PVP system $\epsilon = 0.0028$, which means that our phase angle Ψ depends negligibly on d .

Cracks, and any crazes preceding them, tend to propagate toward a direction which minimizes the local σ_{xy} and thus Ψ . This tendency is especially pronounced for polymer/polymer interfaces when one polymer has a lower Young's modulus and a lower crazing stress than the other.¹¹

At PS/PVP interfaces in symmetrically loaded specimens, an interfacial crack and a craze would be driven toward the PS phase due to the Young's modulus mismatch, resulting in a larger G_c compared with that of the interface itself. We define such a phase angle as positive.

In order to measure the true value of G_c , the testing geometry must therefore have a small negative Ψ , which compensates the modulus mismatch and forces an interfacial crack to propagate at the interface. The asymmetric double cantilever beam geometry (thicker PS beam and thinner PVP beam) used in this study satisfies this small negative Ψ condition, ensuring that we will measure the G_c of the interface itself. More details about the asymmetric double cantilever beam fracture test can be found elsewhere.^{8,11}

(4) **TEM Observation of the Interface Structure and Crack Tip Zone.** We have combined a microtoming method²¹ to produce thin films containing the interface and a copper grid technique²² to allow such microtomed films to be strained in order to observe the fracture mechanisms at the interfaces by TEM.¹⁰ A small piece of the strip was microtomed such that the

plane of the interface was perpendicular to the section and the direction of cutting was parallel to the interface to obtain thin ($\sim 1.0\text{-}\mu\text{m}$) films. Wrinkles in the film caused by microtoming were removed by briefly exposing the film to solvent (toluene/chloroform = 50/50) vapor. The resulting film was then bonded to a ductile copper grid (1×1 mm grid squares), the grid bars of which had been previously coated with PS/PVP block copolymer (PS/PVP = 960/950), by exposure to the vapor of the same solvent mixture for several seconds to ensure good bonding between the grid bars and the film, and then dried at 50°C for 12 h in vacuum to evaporate the solvents and to relax the residual stress.

The resulting grid was strained in tension at a constant strain rate of $\sim 4 \times 10^{-4}/\text{s}$ with a servo-controlled motor drive at room temperature in air. With this strain rate, the craze interface velocity (which is proportional to, but less than, the crack velocity) of this TEM experiment is very close to that of the fracture toughness measurement. The plastic deformation of the copper grid ensures that the strain in the polymer film was retained during the TEM observation. The film was then exposed to iodine vapor at room temperature for 3 h to stain the PVP phase in the film for the TEM observation. PVP forms a complex with iodine,²³ while PS does not, resulting in enhanced electron scattering from the PVP phase. The grid bars surrounding those of a selected squares were carefully cut with a razor blade, and then the film was observed with a (JEOL Model 1200EX) transmission electron microscope operating 120 keV. More details of this technique can be found elsewhere.¹⁰

Results

(1) G_c Measurement. Asymmetric Block Copolymer. Figure 1a shows G_c as a function of Σ for the 580/220 block copolymer. After exhibiting a discontinuous jump at $\Sigma^* = 0.04 \text{ chains/nm}^2$, G_c remained approximately constant in the large Σ regime as shown in Figure 1a. The discontinuous jump at Σ^* is due to a transition in the fracture mechanism from chain pullout ($\Sigma < \Sigma^*$) to crazing ($\Sigma > \Sigma^*$).²⁴ Since Σ_{eff} , which is the number of effectively entangled (load bearing) block copolymer chains per unit area of the interface, remains saturated in the high Σ regime,^{8,24} G_c does not increase with Σ . A more detailed discussion will be found elsewhere.²⁴

Symmetric Block Copolymers. Parts b and c of Figure 1 show G_c as a function of Σ for the 510/540 and 800/870 block copolymers, respectively. In contrast to the results for the asymmetric block copolymer, G_c showed a maximum at $\Sigma \approx 0.2 \text{ chains/nm}^2$, then decreased, and finally reached a constant value for both symmetric block copolymers as shown in parts b and c of Figure 1. Such a maximum in G_c as a function of Σ was also reported by Brown⁴ in the case of PMMA/PS interfaces reinforced with some symmetric PS/PMMA block copolymers. In that investigation, he found the maximum was achieved when the thickness of the deposited block copolymer layer was half the thickness of a PS/PMMA lamella in the bulk, microphase-separated block copolymer. It should be noted that the decrease of G_c after the peak was much larger for 510/540 than for 800/870; the plateau value at large Σ for 510/540 is only $1/4$ of its maximum G_c , while the plateau value for 800/870 is $2/3$ of its maximum G_c .

These results show that there is an optimum Σ for toughening of interfaces with diblock copolymers when these diblock copolymers are symmetric. In order to investigate the reason for such G_c behavior in more detail, further examination of the interface structure is necessary, the results of which are presented in the next section.

(2) Undeformed Structure of an Interface. Asymmetric Block Copolymer. Figure 2 shows the typical PS/PVP interfacial structure with $\Sigma = 0.20 \text{ chains/nm}^2$ of 580/220. Spherical micelles can be seen in the PS side of the interface; these micelles can be seen when $\Sigma > 0.12 \text{ chains/nm}^2$. However, G_c did not show any difference

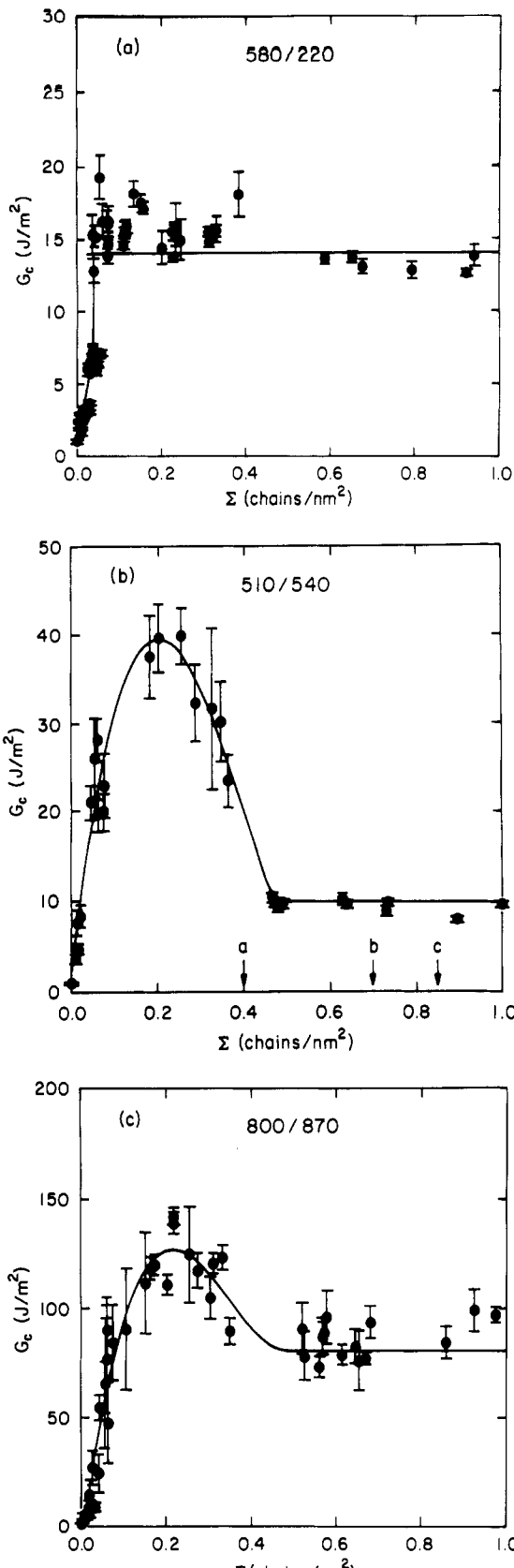


Figure 1. Fracture toughness, G_c , plotted as a function of areal chain density of the block copolymer, Σ . The interfaces are reinforced with (a) 580/220, (b) 510/540, and (c) 800/870. Note that for symmetric block copolymers (510/540 and 800/870) G_c shows a maximum, while for the asymmetric one, G_c remains approximately constant. In Figure 1b, the arrows labeled a-c are the Σ 's at which the micrographs in parts a-c of Figure 3 were taken.

below and above this Σ , indicating that these micelles do not affect G_c .

Symmetric Block Copolymer. In contrast to these results for the asymmetric block copolymer, a well-

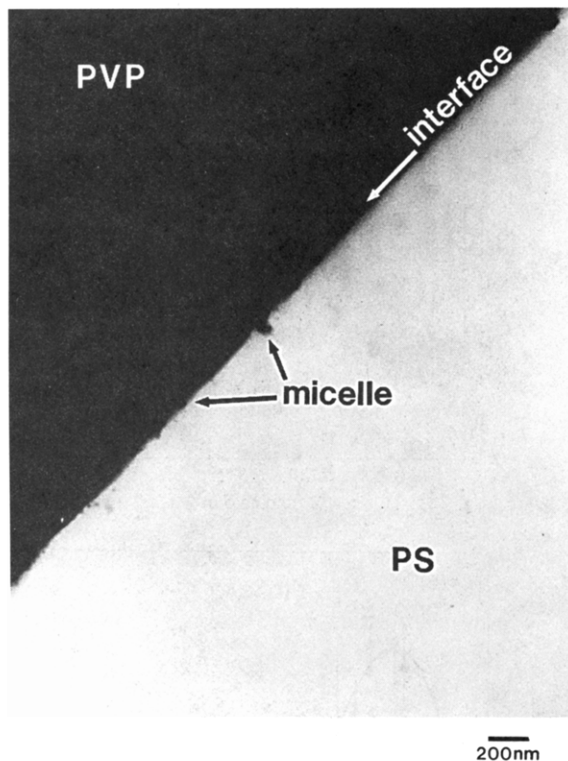


Figure 2. Undeformed structure of an interface reinforced with 580/220 ($\Sigma = 0.20 \text{ chains/nm}^2$). Note that spherical micelles can be seen on the PS side of the interface.

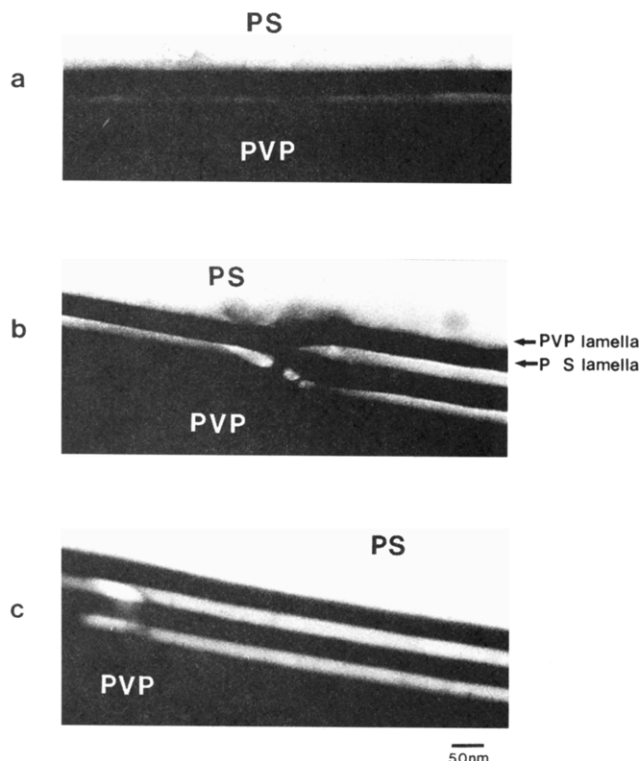


Figure 3. Undeformed structure of an interface reinforced with 510/540, for (a) $\Sigma = 0.40 \text{ chains/nm}^2$, (b) $\Sigma = 0.70 \text{ chains/nm}^2$, and (c) $\Sigma = 0.85 \text{ chains/nm}^2$. Note that the interface is covered with block copolymer lamellae and that the number of lamellar layers depends on Σ . In b a single lamellar layer is connected to a double layer through a lamellar "dislocation".

organized lamellar structure of block copolymer can be seen at the PS/PVP interface at high Σ of symmetric block copolymer (for example, 510/540) as shown in Figure 3a ($\Sigma = 0.4 \text{ chains/nm}^2$). It should be noted that the number of these lamellar layers depends on Σ . We indeed observed

many lamellae of finite size as well as a few micelles at Σ below that required to produce the full coverage of the interface with a lamella. As Σ is increased, single-layer and double-layer lamellar regions are interconnected by a "dislocation" structure as shown in Figure 3b ($\Sigma = 0.7 \text{ chains/nm}^2$), and, finally, at higher Σ a complete double-layer lamellar structure is formed as shown in Figure 3c ($\Sigma = 0.85 \text{ chains/nm}^2$). Similar features were observed for the 800/870 block copolymer. The formation of the lamellar structure introduces one additional type of interface to this system, which may account for the different G_c vs Σ behavior of the interface in these lamella-forming systems.

(3) TEM Analysis of Deformation at and near the Interface. We applied the copper grid method in order to clarify the deformation and fracture mechanisms of these systems. In all cases, we observed a craze on the PS side of the interface as shown in parts a and b of Figure 4 for 580/220 ($\Sigma = 0.20 \text{ chains/nm}^2$) and 800/870 ($\Sigma = 0.20 \text{ chains/nm}^2$), respectively; 510/540 showed similar crazing. The fact that the craze forms only on the PS side of the interface is in accordance with the previous direct TEM observations of crazes at PS/PVP interfaces with smaller Σ of various dPS/PVP block copolymers.¹⁰ These results therefore are a further indication that the crazing stress of PS is lower than that of PVP, consistent with the measurements of these crazing stresses at a typical strain rate of this study (55 MPa for PS and 75 MPa for PVP⁸). The difference in G_c observed for different Σ 's must be caused by different maximum values of craze width (crack opening displacement) before the craze at the crack tip fractures.

(4) Failure Analysis. Asymmetric Block Copolymer. Figure 5a shows the areal density of the 580/220 block copolymer found on the PS or the PVP side, $\Sigma(\text{PS})$ and $\Sigma(\text{PVP})$, as a function of Σ . (Note that $\Sigma = \Sigma(\text{PS}) + \Sigma(\text{PVP})$.) Figure 5a shows that $\Sigma(\text{PVP})$ increased with increasing Σ and then saturated at a value of $\Sigma(\text{PVP}) \approx 0.18 \text{ chains/nm}^2$, while $\Sigma(\text{PS})$ showed a monotonic increase with increasing Σ . These observations indicate that the locus of the fracture plane is between the "brush" of the dPS block of the copolymer adsorbed at the interface and the PS homopolymer as depicted in Figure 6a. It should be noted that while the TEM micrographs show micelles for $\Sigma > 0.12 \text{ chains/nm}^2$, this Σ for first micelle formation is much smaller than that were $\Sigma(\text{PVP})$ saturated ($\Sigma \approx 0.4\text{--}0.5 \text{ chains/nm}^2$). From Figure 4a some part of the craze material can be seen on the PVP side of the fracture surface, even though the majority can be found on the PS side. This observation thus indicates that some spherical micelles located near the interface (see Figure 2) were incorporated in an interfacial craze and then remained on the PVP side when craze breakdown took place.

Symmetric Block Copolymers. Figure 5b shows the fracture analysis for the 510/540 block copolymer. In this system, $\Sigma(\text{PVP})$ saturated at $\Sigma \approx 0.20 \text{ chains/nm}^2$, while $\Sigma(\text{PS})$ monotonically increased with increasing Σ ; this behavior is similar to that of 580/220. Both the saturation value of $\Sigma(\text{PVP})$ and the areal chain density at the saturation in $\Sigma(\text{PVP})$, $\Sigma \approx 0.20 \text{ chains/nm}^2$, are nearly equal to the saturation coverage of the interface with block copolymer (see Appendix). This observation shows that the locus of the fracture plane is between the dPS block brush of the saturated interface and the PS homopolymer at $\Sigma \approx 0.20 \text{ chains/nm}^2$ or between the dPS block brushes of a dPS lamella at larger Σ 's, the latter as depicted in Figure 6b. It should be noted that the fracture plane was not altered by formation of additional lamellae, indicating that the interfacial craze or crack can penetrate into the PVP and PS lamellae but cannot penetrate into the PVP

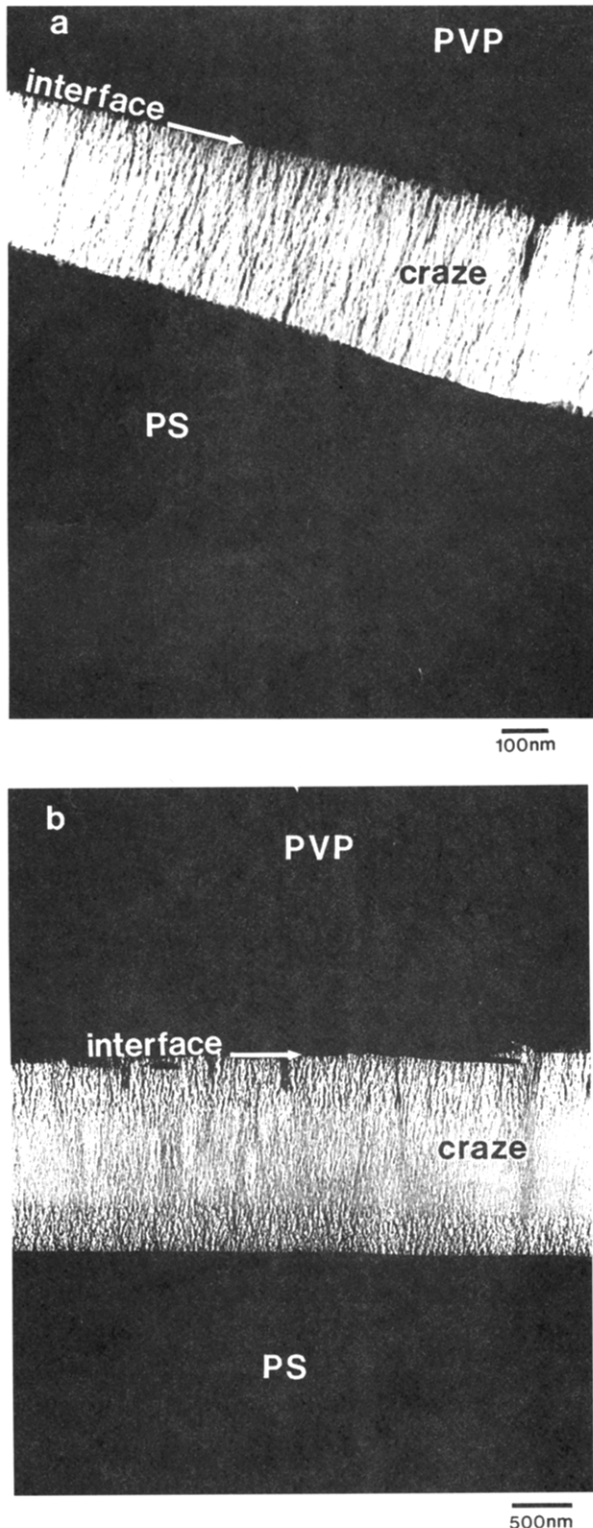


Figure 4. TEM micrograph of the interfacial craze for (a) 580/220 ($\Sigma = 0.20 \text{ chains/nm}^2$) and (b) 800/870 ($\Sigma = 0.20 \text{ chains/nm}^2$). Note that in both cases a craze propagated on the PS side of the interface.

bulk, where the PS (PVP) lamella denotes the PS (PVP) part of the lamellar structure as shown in Figure 6b. This result also implies that the PVP lamella is weaker (less craze and crack resistant) than the PVP bulk. This point will be discussed below.

In contrast to these results for the 510/540 block copolymer, the 800/870 block copolymer showed different behavior. At $\Sigma \approx 0.2 \text{ chains/nm}^2$, $\Sigma(\text{PS})$ began to increase monotonically with increasing Σ and then saturated at $\Sigma \approx 0.5 \text{ chains/nm}^2$ with the saturation value of $\Sigma(\text{PS}) \approx 0.18 \text{ chains/nm}^2$ (see Figure 5c). The Σ at the saturation

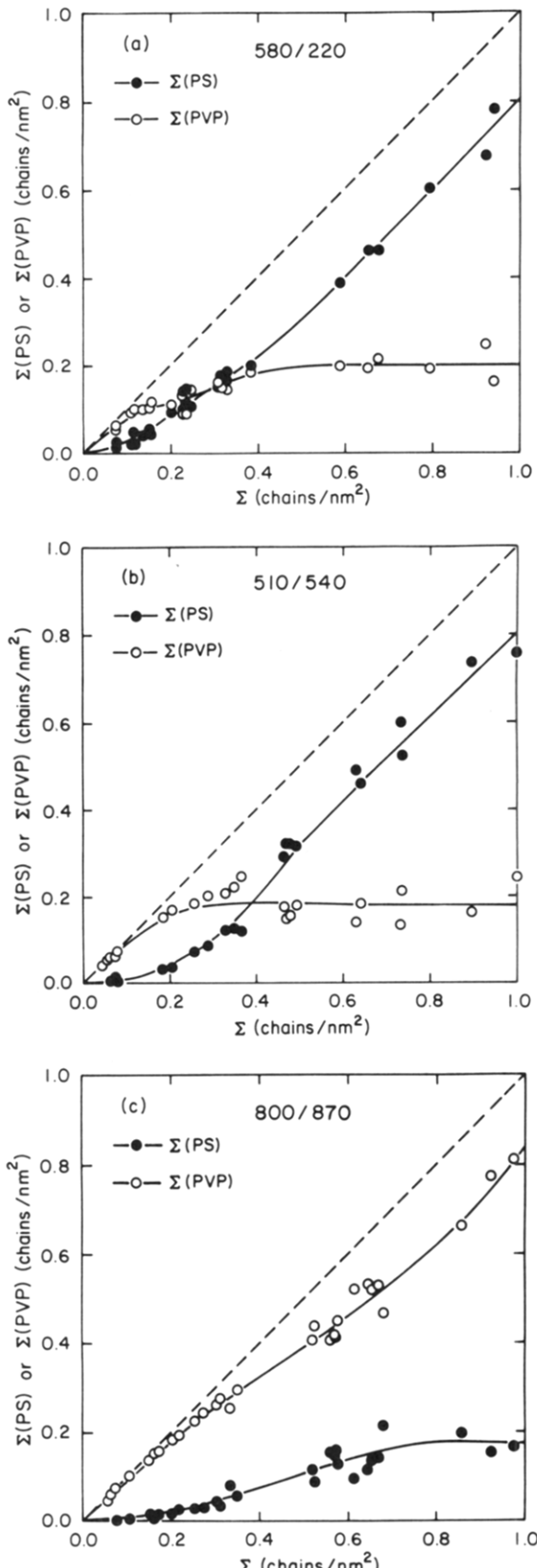


Figure 5. Areal density of the dPS block found on either the PS or PVP side of the fracture surface as a function of Σ for (a) 580/220, (b) 510/540, and (c) 800/870.

coincides with the saturation coverage of the interface with a single block copolymer lamella.

The locus of the fracture plane of the 800/870 system is, however, not as simple as that found in the 510/540 system. Creton et al.⁸ have demonstrated in the study of the same system that, for $\Sigma > 0.03 \text{ chains/nm}^2$, craze breakdown took place at the dPS block/PS homopolymer

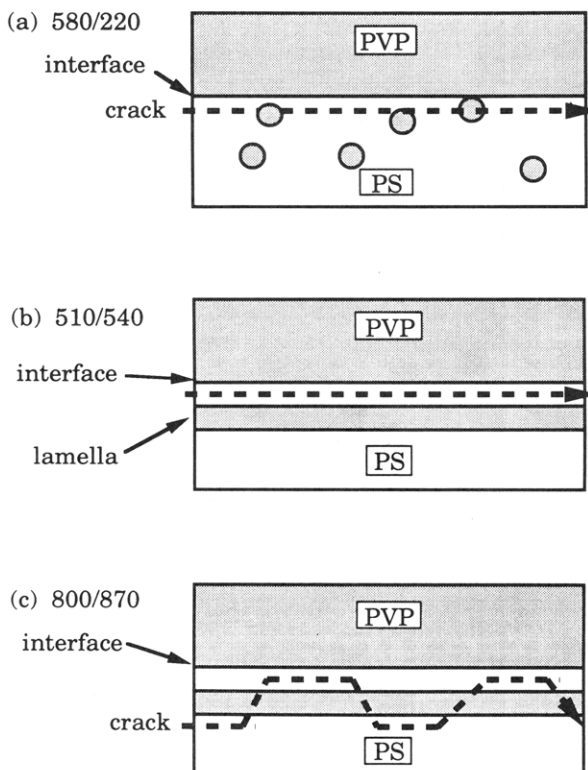


Figure 6. Schematic of the crack trajectory near the interface for (a) 580/220, (b) 510/540, and (c) 800/870 based on the failure analysis. Note that the crack trajectory for the 800/870 block copolymer has an oscillatory characteristic.

interface rather than by chain scission at the joints between the PS and PVP blocks. In the present case, the Σ either at the saturated interface or within the lamella is that for the saturation coverage ($\approx 0.2 \text{ chains/nm}^2$), which is much greater than 0.03 chains/nm^2 , so that the locus of the failure is in the dPS block brush region and not at the joints. Craze breakdown should therefore take place at the interface between either (1) the dPS block brush and PS homopolymer or (2) the dPS block brush and dPS block brush (i.e., within the PS lamella). In the first case, no or very little dPS block should be found on the PS side ($\Sigma(\text{PS}) \sim 0$); on the other hand, in the second case, there should be a constant number of dPS block chains on the PVP side ($\Sigma(\text{PVP}) \approx 0.18 \text{ chains/nm}^2$). Neither of these possibilities can account for the results in Figure 5c.

Discussion

(1) **Trajectory of Fracture of Symmetric Block Copolymers.** There are two possible models to explain the results of the fracture trajectory for the 800/870 block copolymer in the high Σ regime. The first, model I, invokes oscillatory crack propagation, predicting that the crack propagation trajectory oscillates between the outer dPS brush/PS homopolymer interface and the next dPS brush/dPS brush one. The crack propagates along a dPS brush/dPS brush interface (either that between the dPS brush of the saturated PVP interface and the first PS lamella at low Σ or that within a PS lamella at high Σ) for a while but then jumps toward the PS phase and propagates at the interfaces between the dPS brush of the last PS lamella and the PS homopolymer. The second, model II, predicts the crack propagates in the top PVP lamella. Both of these models can account for the results in Figure 5c.

We examined these two models by applying the copper grid method to the 800/870 system ($\Sigma = 0.60 \text{ chains/nm}^2$), where the interface was tilted by 5° from the principal stress axis to introduce a small negative mode phase angle

at the interfacial crack tip¹⁰ so as to force this tip toward the interface (PVP bulk). Note that the sign of the phase angle (negative), and hence the craze trajectory of the copper grid test, corresponds to that for the G_c measurements as discussed earlier. TEM micrographs of the craze and crack of these tilted interfaces are shown in parts a and b of Figure 7. Figure 7a shows a craze tip trajectory in the lamellar region: the interface was reinforced with $\Sigma = 0.60 \text{ chains/nm}^2$ of the 800/870 block copolymer. It is clear from the TEM micrograph that the craze trajectory has the oscillatory characteristic described in model I. In addition, it is obvious from parts b and c of Figure 7 that the PVP lamella remains alternatively on either the PS or the PVP side of the interface, also supporting model I. It should be emphasized strongly that the PVP lamella remaining on either the PS or the PVP side has identically its original thickness (before fracture). From this observation, model II therefore can be eliminated completely. Figure 8 shows an optical microscopic view of the PVP side of the fracture surface (800/870 with $\Sigma = 0.6 \text{ chains/nm}^2$) using the Nomarski contrast technique, where one can see the patches of the dPS/PVP lamellae left on the PVP side of the fracture surface by the oscillatory crack propagation, thus strongly supporting model I. Consequently, the crack trajectory for the 800/870 block copolymer has oscillatory characteristics as shown in Figure 6c and is completely different from that of the 510/540 block copolymer.

The contrasting behavior of the interfacial crack trajectory between the 510/540 block copolymer and the 800/870 block copolymer is expected to arise from the phase angle and the strength of interfacial lamellae themselves. A negative phase angle coming from the ADCB geometry tends to push a craze or a crack tip toward the PVP bulk. Once a craze tip meets a defect in a PVP lamella, the craze tip would tend to penetrate through it and then propagates within the next dPS lamella. Since the PVP lamella of the 510/540 block copolymer will be weaker than that of 800/870 as discussed below, the penetration of the interfacial craze through the PVP lamella of the 510/540 block copolymer will therefore be easier than that of the 800/870 block copolymer.

The tendency for the craze tip to penetrate through the lamellar layer is determined by the phase angle applied. We would thus expect that even for the 800/870 block copolymer a craze or crack tip can penetrate through all the lamellar layers when the phase angle is a sufficiently large negative value and that, furthermore, the craze trajectory for the 510/540 block copolymer can have an oscillatory characteristic when a very small negative phase angle is applied. These features were indeed observed in a separate study by Xiao et al.²⁵

In the case of the 800/870 copolymer, the oscillatory behavior of the crack trajectory appeared under our normal experimental conditions. As the applied crack phase angle is the same for the 800/870 and the 510/540 copolymer reinforced interfaces, the discrepancy is, in our opinion, caused by the difference in strength of the PVP lamellae formed from the two block copolymers as discussed below. In the 800/870 case, it is harder for the propagating craze to cross the PVP lamella to the next dPS lamella, and when small defects in the lamellar structure cause the craze to return to its previously trajectory, it will remain there for a longer time than for the 510/540 (where it presumably crosses back to the dPS lamella immediately), producing the observed oscillatory behavior.

(2) **G_c vs Interface Structure in Symmetric Block Copolymers.** As outlined in the Appendix, the areal chain densities Σ_{sat} corresponding to the saturation coverage of the interface with block copolymer chains are 0.158 and

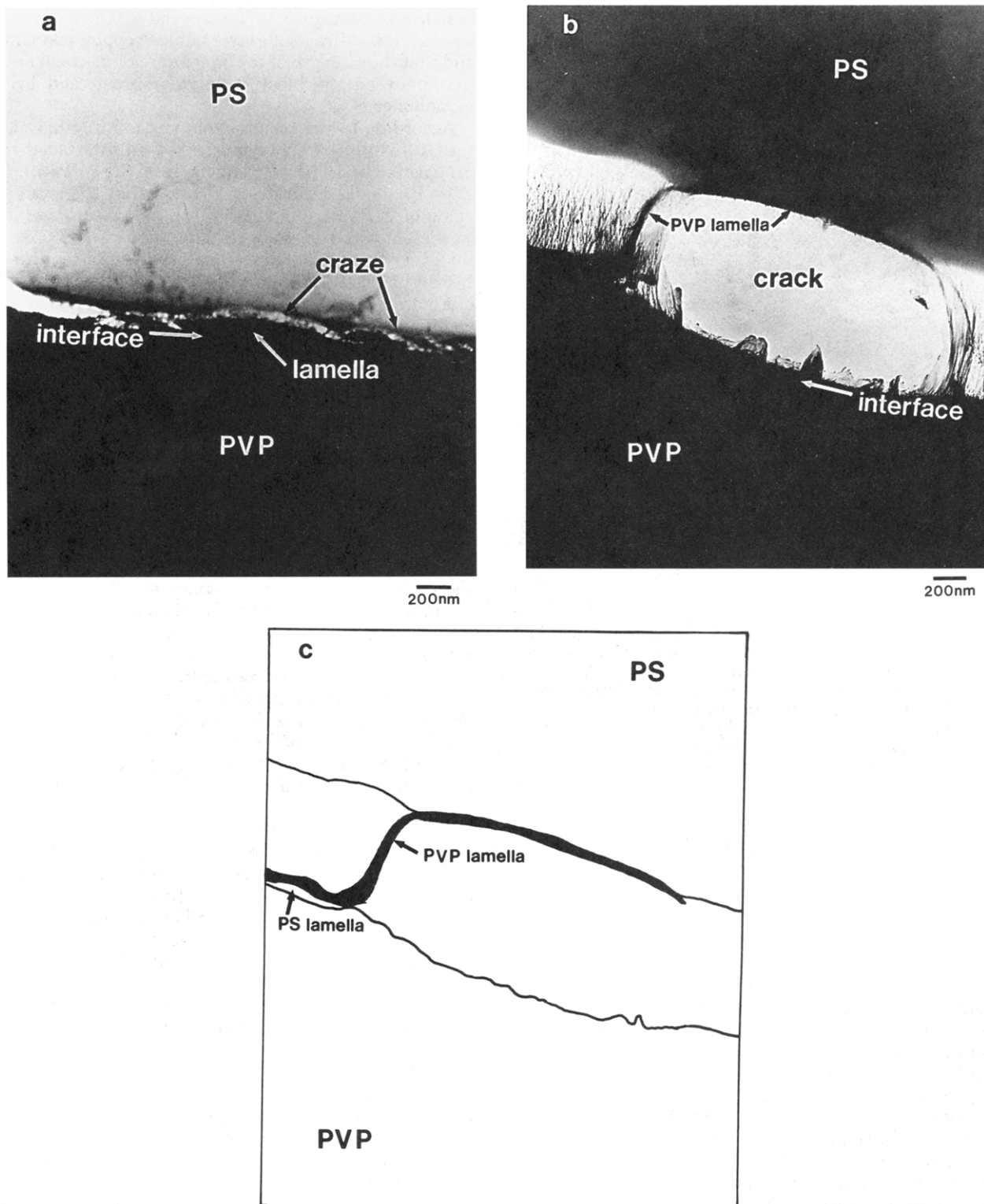


Figure 7. TEM micrographs of the interfacial (a) craze and (b) crack. The interface is reinforced with the 800/870 block copolymer and $\Sigma = 0.60 \text{ chains/nm}^2$. Note that (a) the craze trajectory has oscillatory characteristics and that (b) the block copolymer lamella can be seen on both the PS and PVP sides. Figure 7c is the schematic of b.

0.142 chains/nm² for 510/540 and 800/870, respectively. To estimate the Σ at which lamellae will first form, it is necessary to include any micelles and free block copolymer chains which might be counted in the total Σ by FRES. (Micelles were observed below Σ_{sat} , and the contribution from these micelles should be included in this estimate.) For both cases, these contributions are $\Sigma_{\text{micelle}} \approx 0.01 \text{ chains/nm}^2$ and $\Sigma_{\text{free-chain}} \approx 0$ (see Appendix). Thus the $\Sigma (= \Sigma^\dagger)$ corresponding to the onset of lamellar formation is estimated to be $\Sigma^\dagger \approx 0.17$ and 0.15 chains/nm^2 for 510/540 and 800/870, respectively. (Note that $\Sigma^\dagger = \Sigma_{\text{sat}} + \Sigma_{\text{micelle}}$.) One can obtain Σ_{max} , the areal density at which

G_c showed a maximum from parts b and c of Figure 1. These values, as well as the Σ^\dagger 's, are summarized in the second and third columns of Table II for both block copolymers. In addition, we have estimated $\Sigma^\ddagger (= 3\Sigma_{\text{sat}} + \Sigma_{\text{micelle}})$ corresponding to coverage of the interface with a single layer of block copolymer lamella and from parts b and c of Figure 1 have obtained Σ_{plateau} , the areal density above which G_c remained approximately constant. These values are also listed in the fourth and fifth columns of Table II.

The self-consistent mean-field calculation (SCMF) may be used to estimate Σ_{sat} by using the empirical observation

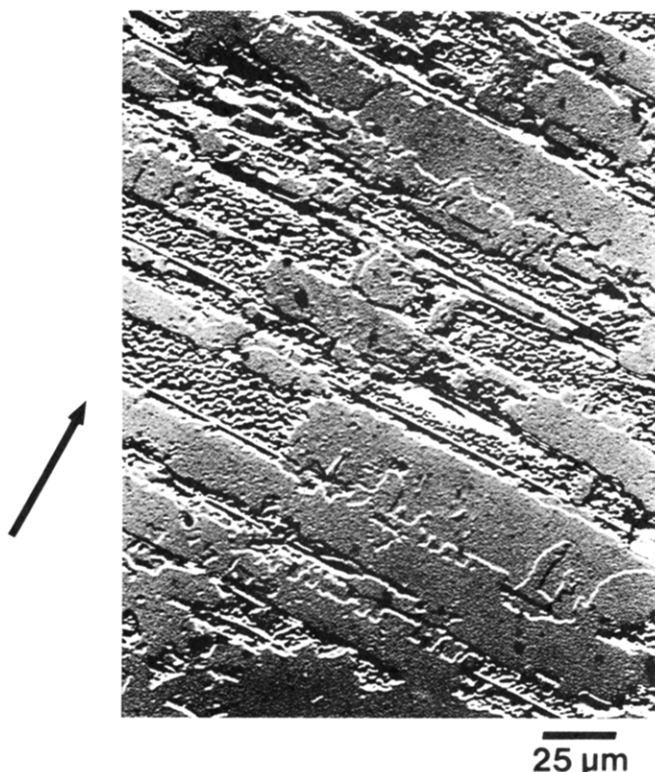


Figure 8. Optical micrograph of the PVP side of the fracture surface using the Nomarski contrast technique. The interface is reinforced with the 800/870 block copolymer and $\Sigma = 0.60$ chains/nm². The arrow represents the direction of crack propagation. Note that the fracture surface has a duplex appearance. The smooth areas are regions where the crack propagated in the dPS lamellae next to the PVP interface, and the rough areas are where it propagated along the outer lamella between the dPS brush and the PS homopolymer.

Table II. Analysis of Interfacial Lamellae of the Symmetric Block Copolymers^a

code	Σ^\dagger	Σ_{\max}	Σ^\ddagger	Σ_{plateau}
510/540	0.17	0.21	0.48	0.50
800/870	0.15	0.19	0.44	0.45

^a All units are in chains/nm².

that PS/PVP block copolymer chains form micelles or lamellae in preference to existing as free block copolymer chains above a block copolymer chemical potential of $\mu_c/k_b T \approx 5.5$.¹⁴ The estimates from the SCMF are $\Sigma_{\text{sat}} \approx 0.10$ and 0.08 chains/nm² for the 510/540 and 800/870 block copolymers, respectively, which are much smaller than the present observations. This comparison is probably caused by the nonequilibrium state of the interface. An excess of block copolymer chains will tend to be squeezed out from the interface in order to reach equilibrium. However, since this process is controlled by diffusion of block copolymer chains and is very slow, the system could not reach equilibrium under the annealing conditions (160 °C for 2 h). Block copolymer chains can therefore remain at the interface with higher Σ compared with the equilibrium value. It should be pointed out that in estimating μ_c for the SCMF calculation, we have assumed that the PVP block of a free block copolymer chain is not collapsed in the PS, which is correct for shorter PVP blocks^{14,16} but not necessarily for long ones. The collapse of the PVP block in the PS bulk would underestimate Σ_{sat} , which can be another reason for the discrepancy.

It is clear in both cases that Σ^\dagger is close to Σ_{\max} , so that the maximum G_c was achieved nearly at the saturation coverage of the interface with block copolymer chains. It is also clear from Table II that $\Sigma^\dagger \approx \Sigma_{\text{plateau}}$, indicating

that the plateau in G_c was achieved when the interface was covered with a single layer of block copolymer lamella and that the strength of the lamellar region is weaker than that between the block copolymer brush and PS homopolymer.

According to the results from the failure analysis for the 510/540 block copolymer, since an interfacial crack propagated in the first PS lamella from the PVP interface, $\Sigma(\text{PVP})$ should saturate at Σ_{\max} , so that the saturation value of $\Sigma(\text{PVP})$ should be ≈ 0.16 chains/nm², which is consistent with the results of Figure 5b. For 800/870, on the other hand, the failure analysis results require that $\Sigma(\text{PS})$ should saturate at Σ_{plateau} , consistent with the results of Figure 5c. The plateau value of $\Sigma(\text{PS})$ is nearly equal to Σ^\dagger , indicating that the crack propagates equally in the dPS lamella and the dPS brush/PS homopolymer interface.

When $\Sigma < \Sigma_{\max}$, the number of entanglements between each block copolymer and its respective homopolymer will increase with increasing Σ , so that G_c increases with increasing Σ as shown in parts b and c of Figure 1.

When $\Sigma_{\max} < \Sigma < \Sigma_{\text{plateau}}$, lamellae of finite size cover the interface. For the 510/540 block copolymer, the interfacial crack tends to propagate within the PS lamella, while for the 800/870 block copolymer the crack propagation trajectory oscillates between the dPS lamella and the dPS brush/PS homopolymer interface. Since the strength of the lamella is smaller than that of the interface fully covered with block copolymer chains for reasons discussed below, G_c decreased with increasing Σ in this regime, consistent with results in parts b and c of Figure 1. As long as those patches of lamella are small ($\Sigma \geq \Sigma^\dagger$), however, they will have little effect on the G_c (cf. the effect of spherical micelles of the 580/220 block copolymer), which probably accounts for the breadth of the G_c peak and the fact that its apparent position Σ_{\max} is somewhat larger than Σ^\dagger .

When $\Sigma > \Sigma_{\text{plateau}}$, the interface was covered with at least one block copolymer lamella plus double lamellae of finite size which are connected through the dislocations as shown in Figure 3b. For the 510/540 block copolymer, since the locus of fracture is still at the first dPS lamella from the PVP interface, additional lamellae cannot affect G_c , consistent with the results in Figure 1b. For the 800/870 block copolymer, G_c also remained approximately constant in this regime, indicating that an interfacial crack propagating in an oscillatory manner along the top (closest to the PS bulk) lamella is unaffected by patches of double lamellae.

One can estimate the fracture toughness $G_c(\text{brush})$ of the dPS brush (interface between dPS block and PS homopolymer) and $G_c(\text{lamella})$ of the dPS lamella (the dPS brush/dPS brush interface). The former corresponds to the maximum G_c (≈ 40 J/m² for 510/540 and ≈ 120 J/m² for 800/870). The $G_c(\text{lamella})$ for the 510/540 block copolymer is G_c at the plateau, since the interfacial crack propagated in the first dPS lamella from the interface as discussed earlier, leading to $G_c(\text{lamella}) \approx 10$ J/m². For the 800/870 block copolymer, $G_c(\text{lamella})$ is estimated to be ≈ 30 J/m² by Xiao et al.,²⁵ where they measured G_c under a large negative phase angle to force a crack to propagate into the first dPS lamella from the PVP interface. The ratio $G_c(\text{brush})/G_c(\text{lamella}) \approx 4$ for both systems. Due to its oscillating crack trajectory, however, the 800/870 block copolymer showed a broader maximum than 510/540, consistent with the observations in parts b and c of Figure 1.

We believe that the low fracture toughness of the lamellae relative to the brush is due to the swelling of lamellae by fractions of the polydisperse homopolymers;

the experimental results demonstrating the swelling are analyzed in the Appendix. The maximum molecular weight of the homopolymer that can swell the lamella is dictated by the macrophase separation between the block copolymer and the homopolymer. Hence, the homopolymer chain swelling its respective lamella is shorter than its respective block due to macrophase separation.²⁶ The entanglement density of such swollen lamellae is thus smaller than that of the interface between the homopolymers which is fully covered with block copolymer chains. Consequently, the strength of the swollen lamellae is weaker than that of the interface fully covered with block copolymer chains. G_c would therefore decrease if an interfacial crack or craze propagates in the swollen lamellae. The strength of the swollen lamellae of the 510/540 block copolymer will be weaker than that of the 800/870 block copolymer, since the 510/540 block copolymer lamellae are swollen by shorter homopolymer chains than the 800/870 block copolymer. Not only the PS lamellae will be affected; the strength of the PVP lamellae of 510/540 and 800/870 should be much less than that of the PVP bulk because of the swelling of these lamellae by short homopolymer. The 800/870 block copolymer lamellae however will be less affected than the 510/540 block copolymer ones, and thus it will require a larger negative phase angle (than that for the 510/540 block copolymer) to allow the craze and crack to "break through" the PVP lamella and to propagate uniformly in the PS lamella next to the PVP interface.

Conclusions

Asymmetric block copolymer (580/220) chains formed spherical micelles on the PS side of the interface at large Σ 's. These block copolymer micelles had no effect on G_c . FRES and TEM observations showed that fracture occurred by crazing in the PS followed by craze breakdown, and the locus of the fracture was the PVP/PS craze interface, between the dPS brush of the copolymer-saturated interface and the PS homopolymer.

In contrast to these results for the asymmetric block copolymer, symmetric block copolymers (510/540 and 800/870) formed lamellae at large Σ 's, at the interface, and this lamellar structure affected G_c . In both cases, after exhibiting a maximum at Σ corresponding to the saturation coverage of the interface with block copolymer chains, G_c began to decrease and finally reached a constant value when the interface was fully covered with one added block copolymer lamella.

TEM observations showed that the fracture mechanism is crazing on the PS side followed by craze breakdown in both cases. FRES analysis revealed that the locus of fracture was within the block copolymer lamellae for the 800/870 system, where the interfacial crack trajectory had an oscillatory characteristic, while fracture took place between the dPS block at the saturated interface and the dPS block of the lamella for the 510/540 system.

These results show that there are limits to the interface toughening that can be produced by adding symmetric diblock copolymers. Adding more block copolymer than needed to saturate the interface actually produces secondary (lamellar) interfaces which are weaker than the original saturated homopolymer one.

Acknowledgment. We gratefully acknowledge that this work was carried out as part of a project of the Cornell Materials Science Center which is funded by the National Science Foundation and benefited from the use of MSC Central Facilities. We also appreciate the important contributions of K. H. Dai in the synthesis of the block

copolymers and Dr. P. Silberzan for stimulating discussions. J.W. is supported by a grant from Showa Denko K.K., Japan.

Appendix: Quantitative Analysis of the Swelling of Interfacial Lamellae

Pure block copolymer films were prepared by microtoming a thin section from a compression-molded sample, which was annealed under conditions (160 °C for 2 h) identical to those used for preparing the PS/PVP fracture samples. TEM observations of lamellae of the pure block copolymer revealed that the total thickness of the interfacial lamellae (see Figure 3) was greater than that of the pure block copolymer by 14% and 23% for the 510/540 and 800/870 block copolymers, respectively. It was also found that the PS and PVP lamellae were swollen equally. This swelling of the interfacial lamellae by homopolymer was caused by the low molecular weight fraction of the polydisperse homopolymers. (Note that the PS and PVP homopolymers used in this study were commercial grade, with the polydispersity indices of 2–3 given in Table I.) It should be noted that the swelling of the interfacial lamellae by the low molecular weight fraction of the homopolymer could be quite an important factor in determining the strength of these lamellae and thus the strength of the interface.

There are two limiting cases for the swelling of lamellae by homopolymer, axial swelling and isotropic swelling.^{27–29} The axial swelling case occurs when the lamellae are swollen only in their axial direction (perpendicular to the interface); i.e., no swelling occurs in the lateral direction (parallel to the interface). Under axial swelling conditions, the homopolymer is located in the center of its respective lamella. Axial swelling is observed when the polymerization index of the homopolymer swelling the lamellae is relatively large. On the other hand, the isotropic swelling case occurs when the lamellae are isotropic swollen, i.e., equally parallel and perpendicular to the interface. Under isotropic swelling conditions, the homopolymer is distributed uniformly in its respective lamella. Isotropic swelling is observed when the polymerization index of the homopolymer is much smaller than the block of the block copolymer. Since the polydisperse homopolymers in this study contain polymer fractions both larger and smaller than the respective block of the block copolymer, it is not clear *a priori* which of these limits, isotropic or axial swelling, is appropriate to describe our experiments.

One can examine the location of the homopolymer in its respective lamella by comparing results from FRES with those from TEM. The areal chain density of the block copolymer at the interface, Σ , can be calculated from TEM micrographs of the interface based on either the axial or the isotropic swelling model; these Σ 's can then be compared with Σ measured by FRES.

The areal chain density of the block copolymer near the interface measured by FRES is given by:

$$\Sigma = \Sigma_{\text{lamella}} + \Sigma_{\text{micelle}} + \Sigma_{\text{free-chain}} \quad (\text{A-1})$$

where Σ denotes the total areal chain density of the block copolymer, and Σ_{lamella} , Σ_{micelle} , and $\Sigma_{\text{free-chain}}$ denote the contributions from lamellae, micelles, and free chains, respectively. Here, Σ is defined by:

$$\Sigma = \int_{-\infty}^{\infty} n(x) dx \quad (\text{A-2})$$

x and $n(x)$ denote a distance from the interface and a number density of block copolymer chains located between x and $x + dx$ with analogous relations for Σ_{lamella} , Σ_{micelle} , and $\Sigma_{\text{free-chain}}$.

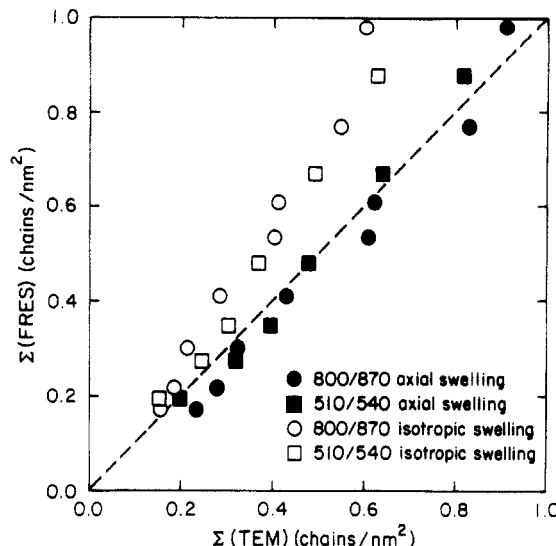


Figure 9. Examination of the swelling of interfacial lamellae based on the axial and isotropic swelling models. The $\Sigma(\text{TEM})$ values for the closed symbols, squares for the 510/540 and circles for the 800/870, are calculated based on the axial swelling model. On the other hand, those for the open symbols are calculated based on the isotropic swelling model. Note that the axial swelling model accounts well for the swelling of interfacial lamellae.

The quantity of free block copolymer chains in either the PS or the PVP phase is completely negligible, since the critical micelle concentrations of these block copolymers on either side are very low as discussed in a separate study,¹⁰ giving $\Sigma_{\text{free-chain}} \approx 0$. Block copolymer chains forming micelles can be evaluated from quantitative image analysis of TEM micrographs by measuring the number and size of the micelles, and this analysis revealed that the contribution from these micelles was $\Sigma_{\text{micelle}} \approx 0.01$ chains/ nm^2 in the large Σ regime and $\Sigma > 0.15$ chains/ nm^2 for both the 510/540 and 800/870 block copolymers. Σ_{lamella} can also be estimated from a quantitative image analysis of TEM micrographs and is given by:

$$\Sigma_{\text{lamella}} = \Sigma_{\text{sat}} + 2(n + p_{\text{top}})\Sigma_{\text{sat}} \quad (\text{A-3})$$

where n and p_{top} denote the number of full lamellae covering the interface and the fractional coverage with lamellae of finite size, respectively. The first term on the right-hand side of eq A-3 corresponds to the saturation coverage of the interface with block copolymer chains, and the second term corresponds to the contribution from the lamellae. Here we have assumed that the top surface of a lamella, including one of finite size, has the same areal chain density of Σ_{sat} . From volumetric considerations, one can evaluate Σ_{sat} to be given by:

$$\Sigma_{\text{sat}} = L_0 \rho_{\text{bcp}} N_A / 2M_{\text{bcp}} \quad \text{axial swelling} \quad (\text{A-4})$$

$$\Sigma_{\text{sat}} = L_0 \rho_{\text{bcp}} N_A R^2 / 2M_{\text{bcp}} \quad \text{isotropic swelling} \quad (\text{A-5})$$

$$R = L_0 / L \quad (\text{A-6})$$

where ρ_{bcp} and M_{bcp} denote respectively the density and

molecular weight of the block copolymer, and N_A denotes Avogadro's number. L_0 and L represent repeating periods of a pure block copolymer lamella and an interfacial one, respectively. Experimentally we determined n and p_{top} from TEM micrographs: we took 12 TEM micrographs at a magnification of 10 000 times, covering a length of 120 μm of the interface; analysis of these micrographs allowed us to achieve good statistics in evaluating p_{top} .

Figure 9 shows the examination of the swelling models, where $\Sigma(\text{FRES})$ was obtained from FRES and $\Sigma(\text{TEM})$ was estimated from TEM micrographs based on both the axial and the isotropic swelling models. It is clear from Figure 9 that the axial swelling model accounts well for the FRES results, while the isotropic swelling model cannot account for the FRES results at all, indicating that the homopolymer chains swelling their respective lamella are localized in the center of the lamella.

References and Notes

- (1) Fayt, R.; Jérôme, R.; Teyssié, Ph. *J. Polym. Sci., Polym. Phys. Ed.* 1989, 27, 775.
- (2) Fayt, R.; Teyssié, Ph. *Polym. Eng. Sci.* 1989, 29, 538.
- (3) Brown, H. R.; Deline, V.; Green, P. F. *Nature* 1989, 341, 221.
- (4) Brown, H. R. *Macromolecules* 1989, 22, 2859.
- (5) Brown, H. R. *Macromolecules* 1991, 24, 2752.
- (6) Xu, D. B.; Hui, C. Y.; Kramer, E. J.; Creton, C. *Mech. Mater.* 1991, 11, 257.
- (7) Creton, C.; Kramer, E. J.; Hadzioannou, G. *Macromolecules* 1991, 24, 1846.
- (8) Creton, C. F.; Kramer, E. J.; Hui, C. Y.; Brown, H. R. *Macromolecules* 1992, 25, 3075.
- (9) Hui, C. Y.; Ruina, A.; Creton, C.; Kramer, E. J. *Macromolecules* 1992, 25, 3948.
- (10) Washiyama, J.; Creton, C.; Kramer, E. J. *Macromolecules* 1992, 25, 4751.
- (11) Brown, H. R. *J. Mater. Sci.* 1990, 25, 2791.
- (12) Cao, H. C.; Dagleish, B. J.; Evans, A. G. *Closed Loop* 1990, 23, 3929.
- (13) Shull, K. R.; Winey, K. I.; Thomas, E. L.; Kramer, E. J. *Macromolecules* 1991, 24, 2748.
- (14) Shull, K. R.; Kramer, E. J.; Hadzioannou, G.; Tang, W. *Macromolecules* 1990, 23, 4780.
- (15) Shull, K. R.; Kramer, E. J. *Macromolecules* 1990, 23, 4769.
- (16) Dai, K. H.; Kramer, E. J.; Shull, K. R. *Macromolecules* 1992, 25, 220.
- (17) Feldman, L. C.; Mayer, J. W. *Fundamentals of Surface and Thin Film Analysis*; North-Holland: Amsterdam, The Netherlands, 1986.
- (18) Mills, P. J.; Green, P. F.; Palmstrom, C. J.; Mayer, J. W.; Kramer, E. J. *J. Appl. Phys. Lett.* 1984, 45, 958.
- (19) Shull, K. R. Ph.D. Thesis, Cornell University, Ithaca, NY, 1990.
- (20) Rice, J. R. *J. Appl. Mech.* 1988, 55, 98.
- (21) Beahan, P.; Bevis, M.; Hull, D. *Philos. Mag.* 1971, 24, 1267.
- (22) Lauterwasser, B. D.; Kramer, E. J. *Philos. Mag.* 1979, A39, 469.
- (23) Aronson, S.; Wilensky, S. B. *J. Polym. Sci., Polym. Chem. Ed.* 1988, 26, 1259.
- (24) Washiyama, J.; Kramer, E. J.; Hui, C. Y. *Macromolecules* 1993, 26, 2928.
- (25) Xiao, F.; Hui, C. Y.; Washiyama, J.; Kramer, E. J., to be submitted for publication.
- (26) Inoue, T.; Soen, T.; Hashimoto, T.; Kawai, H. *Macromolecules* 1970, 3, 87.
- (27) Hashimoto, T.; Tanaka, H.; Hasegawa, H. *Macromolecules* 1990, 23, 4378.
- (28) Tanaka, H.; Hasegawa, H.; Hashimoto, T. *Macromolecules* 1991, 24, 240.
- (29) Winey, K. I.; Thomas, E. L.; Fetter, L. J. *Macromolecules* 1991, 24, 6182.